Engineering Optimization

ISSN: (Print) (Online) Journal homepage: https://www.tandfonline.com/loi/geno20

A novel particle swarm optimization optimal control parameter determination strategy for maximum power point trackers of partially shaded photovoltaic systems

Ali M. Eltamaly

ENGINEERING OPTIMIZATION
https://doi.org/10.1080/0305215X.2021.1890724

Taylor & Francis
Taylor & Francis Group

Check for updates

A novel particle swarm optimization optimal control parameter determination strategy for maximum power point trackers of partially shaded photovoltaic systems

Ali M. Eltamaly [a,b,c]

[a]Sustainable Energy Technologies Center, King Saud University, Riyadh, Saudi Arabia; [b]Electrical Engineering Department, Mansoura University, Mansoura, Egypt; [c]K.A. CARE Energy Research and Innovation Center, Riyadh, Saudi Arabia

ABSTRACT
This article introduces a novel strategy for determining the optimal control parameters of particle swarm optimization (PSO) for the shortest convergence time and lowest failure rate of photovoltaic (PV) maximum power point tracker (MPPT) systems. This strategy is used offline to determine these parameters and then the control system uses them in the online MPPT. The strategy uses two nested particle swarm optimization (NESTPSO) search loops: the inner one involves the PV system and the outer one uses the inner PSO as a fitness function. The control parameters and swarm size of the inner PSO loop are used as optimization variables in the outer PSO loop. This strategy can be used not only for PSO but also for all other optimization techniques. The simulation and experimental results obtained using the NESTPSO strategy show a great reduction of 77–681% in convergence time and failure rate compared to 10 benchmark strategies, proving the superiority of this technique.

ARTICLE HISTORY
Received 6 May 2020
Accepted 8 February 2021

KEYWORDS
Photovoltaic; MPPT; particle swarm optimization; convergence time; failure rate

1. Introduction

Partial shading in photovoltaic (PV) arrays creates more than one peak in the power–voltage (P-V) characteristics. The global peak (GP) has the highest power peak, while the local peaks (LPs) have the lowest power. The maximum power point tracker (MPPT) is used to track the GP. Many swarm optimization techniques have been used to perform the MPPT function in cases of uniform irradiance or partial shading conditions (PSC) (Eltamaly *et al.* 2020; Eltamaly and Farh 2019; Titri *et al.* 2017). All of these techniques have control parameters and swarm sizes, which considerably affect their convergence time, t_c, and failure rate, *FR*. So far, there have been no studies in the literature on determining the optimal values of the control parameters; instead, most of the previous research involves tuning these parameters. Inaccurate estimation of these parameter values may cause an increase in the failure rate and convergence time, which will adversely affect the convergence performance (Ahmed and Salam 2014; Eltamaly *et al.* 2020; Sangeetha, Babu, and Rajasekar 2016).

Reducing the convergence time of the particle swarm optimization (PSO) will add great value to its use in the MPPT of PV systems and other applications, and was the motivation for this study. Owing

CONTACT Ali M. Eltamaly eltamaly@ksu.edu.sa

to its simplicity, robustness and popularity, PSO has been used in this study to follow the GP of PV energy systems. The convergence time and failure rate can be considerably reduced if PSO or other soft computing techniques function with optimal control parameters (Eltamaly *et al*. 2020; Farh *et al*. 2019; Hou *et al*. 2016). A higher failure rate and convergence time of the MPPT of the PV array during online operation may cause instability and a reduction in the generated energy. These two factors are functions of the control parameters and the swarm size of the PSO (Eltamaly 2018; Farh, Eltamaly, and Othman 2018). Although the PSO control parameters and the swarm size have a substantial effect on the failure rate and convergence time, there is no previous literature on how to determine their optimal values. Most of the studies using PSO or other soft computing techniques estimated these values from other applications or after tuning (Eltamaly 2015a, 2015b; Eltamaly, Farh, and Saud 2019; Grefenstette 1986; Mason, Duggan, and Howley 2018). Early efforts were made in 1986 by linearly changing the genetic algorithm control parameters to obtain the minimum convergence time and use these parameters (Grefenstette 1986). This tuning technique selects the minimum available convergence time parameters, which will not lead to the optimal solution. Moreover, to perform this tuning technique, three nested loops are required, which will take more iterations than the number needed for nested particle swarm optimization (NESTPSO). Later, in 2018, the results obtained from running the PSO were used to train a neural network, which was used to obtain the PSO weight parameter, ω, associated with fast convergence (Mason, Duggan, and Howley 2018). The idea introduced in this article is used only to obtain the best value of the inertia weight parameter, ω, but not to obtain the other control parameters or swarm size (SS). Moreover, the resulting value is the best available from training the neural network, which may not be the optimal solution (Mason, Duggan, and Howley 2018). The optimal swarm size for all metaheuristic techniques has never been discussed in the literature; most previous studies used the number of particles equal to the number of peaks in the P-V curves, without any justification (Eltamaly 2015a, 2015b; Eltamaly *et al*. 2020; Eltamaly, Farh, and Saud 2019). This poor estimation of the PSO control parameters and swarm size may cause an increase in the failure rate and/or prolong the convergence time, which can adversely affect the performance of PV systems.

This objective of this article is to evaluate the optimal values of the PSO control parameters when PSO is used for to track the GP of a PV array. This strategy can be used with any other soft computing optimization technique. The strategy uses two nested PSO loops: the outer PSO loop optimizes the control parameters used in the inner PSO loop to achieve the lowest convergence time and failure rate as the objective function. Meanwhile, the inner PSO loop is used to obtain the optimal duty ratio of the boost converter. So, the inner PSO loop is counted as a fitness function to the outer PSO loop, where it optimizes the control parameters of the inner PSO loop to obtain the lowest values of the failure rate and the convergence time. The PV system is used as a fitness function for the inner PSO loop, where it uses the control parameters suggested from the outer PSO loop to obtain the optimal duty ratio associated with the maximum power. This nested PSO strategy is called NESTPSO; it is performed offline to determine the optimal values of the PSO control parameters and use them with the regular online PSO MPPT of the PV systems. To the author's knowledge, no previous research has been conducted to determine the optimal PSO control parameters and swarm size for PSO. Moreover, the strategy introduced in this article, using PSO as an MPPT in a PV system or any other application, does not appear in the literature. This article will help researchers, designers and experts working in the field of swarm optimization to improve the performance of all optimization techniques in all real-world applications.

This article presents the components of the PV system and their detailed description in Section 2. The detailed operation of PSO in the MPPT of the PV system application is shown in Section 3. A detailed description of NESTPSO and how it is used to determine the PSO control parameters is given in Section 4. The simulation results of NESTPSO and a detailed comparison with benchmark strategies are presented in Section 5. Experimental work showing the prototype used to validate the proposed strategy is demonstrated in Section 6. Section 7 presents the conclusions from this study.

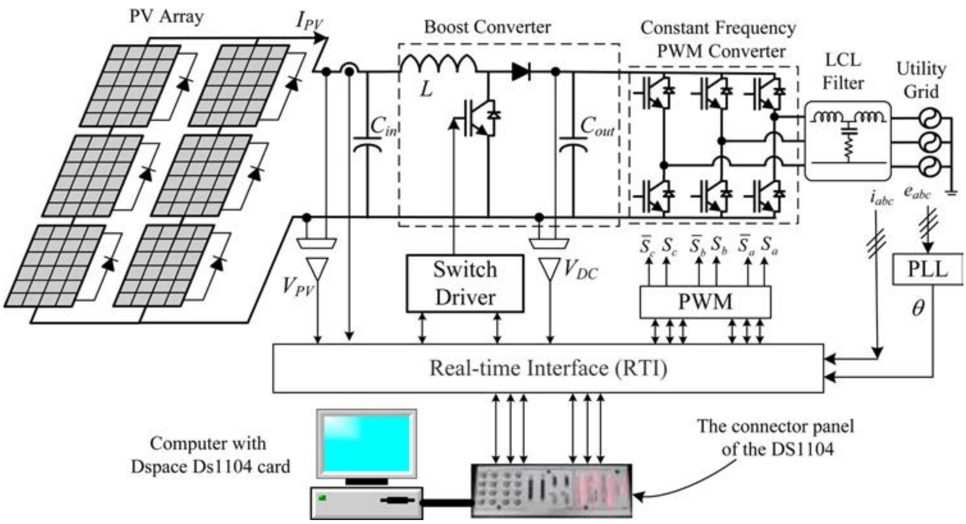

Figure 1. Circuit of a photovoltaic (PV) system with a maximum power point tracker (MPPT). PWM = pulse-width modulation; PLL = phase-locked loop.

2. MPPT of PV system concepts

The relationship between the power generated by the PV arrays and the PV array terminal voltage shows nonlinear characteristics. These nonlinear characteristics need to be tracked effectively to determine the optimal direct current (DC) voltage using DC/DC converters to control the terminal voltage of the PV array. As shown in Figure 1, a boost converter is used to control the terminal voltage of the PV array. The DC-link voltage is connected to a three-phase pulse-width modulation (PWM) inverter to integrate the PV system with the utility grid (Lakshmi and Hemamalini 2018). The PSO MPPT technique and the control of three-phase PWM are achieved using MATLAB® code and Simulink®, using a dSPACE DS1104 R&D Controller Board to control the system (Figure 1).

The PSO technique uses the boost converter to track the maximum power from PV energy systems. The relationship between the input–output voltages and the duty ratio of the boost converter is shown in Equation (1) (Eltamaly, Farh, and Al-Saud 2019; Eltamaly, Al-Saud, and Abokhalil 2020a, 2020b). Based on this equation, the variation in the generated power and duty is shown in Figure 2.

$$V_{DC}/V_{PV} = 1/(1-d) \tag{1}$$

where V_{PV}, V_{DC} and d are the input, output and duty ratio of the boost converter, respectively.

3. PSO MPPT technique of PV energy systems

The PSO technique is inspired by the behaviour of flocks of fish and birds, swarms and shoals searching for food, and is used to determine optimal solutions for multi-dimensional problems. This technique was introduced by Kennedy and Eberhart (1995). The operating principle of this technique is to use several particles to search for the optimal solution in the search space of the optimization problem through consecutive movements of particles. In each new iteration, the particles obtain their movement from their own previous experience and the experience of the swarm, which are called self experience and social experience, respectively. The PSO search performance is determined using Equations (2) and (3). A compromise should be reached between the values of c_l and c_g to achieve a balance between the self and social searches. The velocity of each particle will be added to the

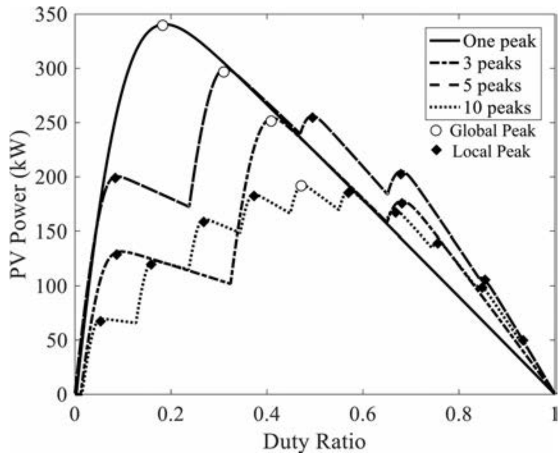

Figure 2. Relationship between the output power and the duty ratio boost converter for a photovoltaic (PV) array for different operating conditions.

previous position of particles ${d_j}^k$ to obtain the new positions of the particles, ${d_{j+1}}^k$ (Eltamaly, Farh, and Abokhalil 2020).

$$ {v_{j+1}}^k = \omega\, {v_j}^k + c_l r_l (d_{best}^k - d_j^k) + c_g r_g (G_{best} - d_j^k) \tag{2} $$

$$ {d_{j+1}}^k = {d_j}^k + v_{j+1}^k \tag{3} $$

where ω, c_l and c_g are the PSO control parameters. d_{best}^k is the personal best position of particle k, G_{best} is the global best position, r_l and r_g are random values between [0 1], and the counter j is the iteration order of the PSO.

4. New proposed NESTPSO strategy

As discussed in Section 1, the PSO control parameters and swarm size have a great effect on the performance of the PSO, based on the convergence time and failure rate. Inaccurate estimation of these parameters will adversely affect the performance of the PSO. Knowing the importance of these parameters on the performance of the PSO, this article introduces a new strategy (NESTPSO) to determine these parameters offline and uses the results in online applications of the PSO in MPPT of the PV system. To the author's knowledge, this study introduces for the first time a strategy that can determine the optimal values of control parameters of PSO or any other swarm optimization technique in any real-world application. NESTPSO has two nested loops, the outer and inner PSO loops, as shown in Figures 3 and 4, respectively. The outer PSO loop of NESTPSO optimizes the PSO control parameters of the inner PSO loop to obtain the optimal values of these parameters for the minimum failure rate and convergence time of the inner PSO loop. So, the control parameters of the inner PSO loop are used as optimization variables in the outer PSO loop. The inner PSO loop obtains the values of control parameters from the outer PSO loop and it (the inner PSO loop) uses these parameters to run the MPPT of the PV system N_{av} times to avoid the random nature of the PSO technique. The results from the inner PSO loop are the average convergence time and failure rate. The convergence time is the time consumed to reach the final convergence, which is equal to the number of iterations of the inner PSO loop, N_s, used to obtain the steady state of PSO, multiplied by the swarm size of the inner PSO loop, SS_i, and the sampling rate t_s, as shown in Equation (4):

$$ t_c = N_s * SS_i * t_s \tag{4} $$

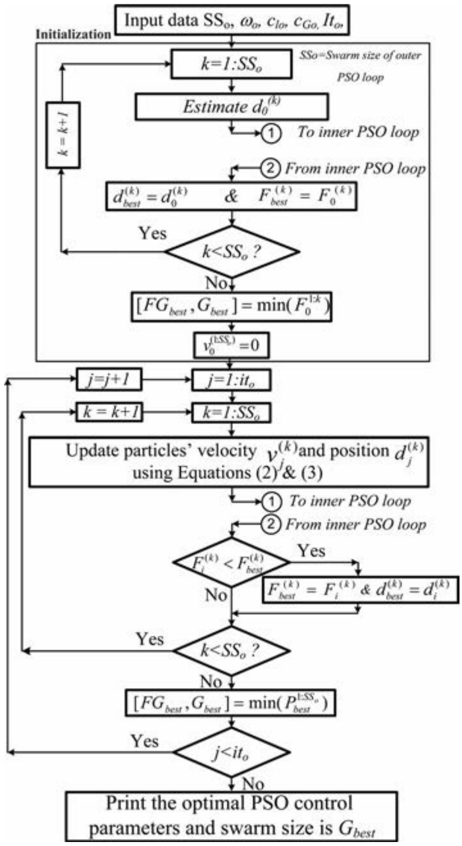

Figure 3. Flowchart of the outer particle swarm optimization (PSO) loop of nested particle swarm optimization (NESTPSO) for determining parameters of the PSO maximum power point tracker (MPPT) of photovoltaic (PV) systems.

where N_s is the average number of iterations consumed to obtain the final solution of the inner PSO loop. This value can be obtained by accumulating the number of iterations consumed to obtain the convergence each time the MPPT inside the inner PSO loop is executed divided by the total number of averaging cycles N_{av}, as shown in detail in the flowchart of the inner PSO loop of NESTPSO in Figure 4.

The failure rate is used to measure the number of times the PSO failed to capture the GP divided by N_{av}:

$$FR = (N_{FR}/N_{av}) * 100 \tag{5}$$

where N_{FR} is the number of occurrences of failure.

The values of t_c and FR are used to determine the objective function, F:

$$F = M * FR + t_c \tag{6}$$

where M is a weighting constant used to give the failure rate some degree of importance, where a higher value of M reduces the value of the failure rate and *vice versa*.

4.1. NESTPSO steps

The steps showing the logic of NESTPSO in determining the optimal PSO control parameters and swarm size as an MPPT of the PV system are shown in the following points and shown in detail in

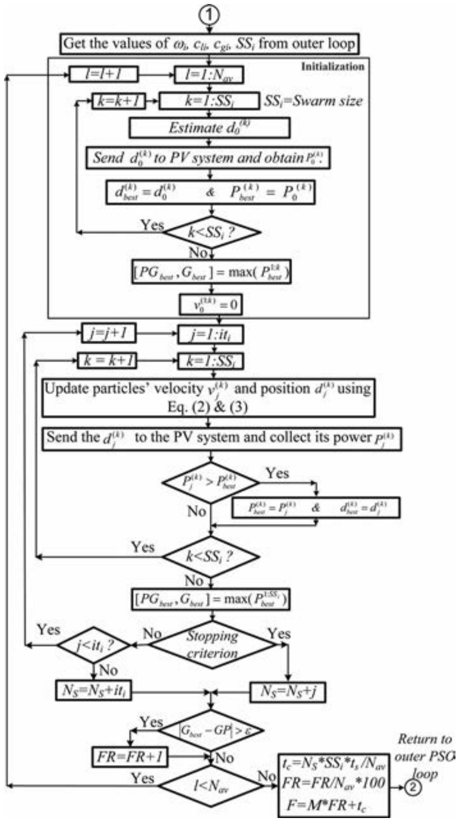

Figure 4. Flowchart of the inner particle swarm optimization (PSO) loop of nested particle swarm optimization (NESTPSO) for determining parameters of the PSO maximum power point tracker (MPPT) of photovoltaic (PV) systems.

Figure 3, where the suffix 'o' is used to represent the outer PSO loop and the suffix 'i' to represent the inner PSO loop of NESTPSO.

Step out 1: Set the control parameters and swarm size of the outer PSO loop (ω_o, c_{lo}, c_{go} and SS_o).

Step out 2: Initiate the values of the particles of the outer PSO loop $(d_0^k)_o$ that contain the control parameters and swarm size of the inner PSO loop, as shown in (7):

$$(d_0^k)_o = [d_0^1 \quad d_0^2 \quad \ldots \quad d_0^{SS_o}] = \begin{Bmatrix} (\omega_0^1)_i & (\omega_0^2)_i & \ldots & (\omega_0^{SS_o})_i \\ (c_{l0}^1)_i & (c_{l0}^2)_i & \ldots & (c_{l0}^{SS_o})_i \\ (c_{g0}^1)_i & (c_{g0}^2)_i & \ldots & (c_{g0}^{SS_o})_i \\ (SS_0^1)_i & (SS_0^2)_i & \ldots & (SS_0^{SS_o})_i \end{Bmatrix} \tag{7}$$

Step out 3: Send the values $(d_0^k)_o$ to the inner PSO loop and obtain the objective function, F_0^k, as shown in (6).

Step out 4: Set the initial values of the particles' best positions, $(d_{best}^k)_o = d_0^k$ and $F_{best}^k = F_0^k$. Select the minimum objective function of F_0^k and save its value and position to FG_{best} and G_{best}.

Step out 5: Set the initial velocity to zero, $({v_0}^k)_o = 0$.

Step out 6: Use the values of the global best (G_{best}), the private best positions of each particle, $(F_{best}^k)_o$, $({v_j}^k)_o$, and the new positions of particles, $({d_j}^k)_o$, from (2) and (3).

Step out 7: Determine the fitness function $(F_j^k)_o$ by applying the particles' positions, $({d_j}^k)_o$, to the PV system.

Step out 8: Check whether the value of the particles, $(F_j^k)_o$, is greater than the stored value, $(F_{best}^k)_o$, and update $(F_{best}^k)_o$ and $(d_{best}^k)_o$. Update FG_{best} and $G_{best,o}$ by comparing their previous values with min $(F_{best}^k)_o$.

Step out 9: If the stopping criterion is valid, stop and print the optimal PSO control parameters and swarm size, $G_{best,o}$. If it is not valid, go to **Step out 6**.

The following steps show the inner PSO loop.

Step in 1: Receive the values of PSO control parameters and swarm size from the outer PSO loop (ω_i, c_{li}, c_{gi} and SS_i).

Step in 2: Set $N_{av} = 10{,}000$, $N_s = 0$ and $FR = 0$.

Step in 3: Start with the initial values of particles (duty ratios) $d_0^{1:SS_i} = [d_0^1 \quad d_0^2 \ldots .d_0^k \ldots .d_0^{SS_i}]$; send these values one by one to the PV system and collect the power, P_0^k.

Step in 4: Set $d_{best}^k = d_0^k$, $P_{best}^k = P_0^k$ and $PG_{best} = \max(P_0^{1:SS_i})$, and the corresponding duty ratio G_{best}.

Step in 5: Set the initial velocity to zero (${v_0}^{1:SS_i} = 0$).

Step in 6: Use the values of G_{best} and d_{best}^k to determine ${v_{j+1}}^k$ and ${d_{j+1}}^k$ of particles from (2) and (3).

Step in 7: Send the new values of ${d_{j+1}}^k$ obtained from **Step in 6** to the PV system and collect ${P_{j+1}}^k$.

Step in 8: Check whether ${P_{j+1}}^k > P_{best}^k$ and update the particles' best values and positions, P_{best}^k and d_{best}^k, respectively. Then, update PG_{best} and G_{best} so that if the $\max(P_{best}^k) > PG_{best}$ then $PG_{best} =$ max $(P_{best}^k)_i$ and $G_{best,i} = (d_{best}^k)_i$.

Step in 9: If the stopping criterion is validated, set $N_s = N_s + j$, then go to **Step in 12**; otherwise, go to **Step in 10**.

Step in 10: If $j \geq it_i$, then $N_s = N_s + it_i$, then go to **Step in 12**; otherwise, go to **Step in 11**.

Step in 11: If the stopping criterion is not validated and $j \leq it_i$, then $j = j + 1$, then go to **Step in 6**.

Step in 12: Check that the solution is not the GP using the condition (if $|G_{best} - GP| > \varepsilon$), then $FR = FR + 1$, where ε is a predefined tolerance; $\varepsilon = 0.001$ in the simulation.

Step in 13: If the average number of simulation times is less than N_{av}, go to **Step in 3**; otherwise, go to **Step in 14.**

Step in 14: Calculate the FR, t_c and objective function from (6), $FR = FR/N_{av} * 100$, $t_c = N_s * SS_i * t_s/N_{av}$, $F = M * FR + t_c$.

Step in 15: End of the inner PSO loop; go to the outer one.

4.2. Stopping criteria

The execution of the NESTPSO code should be terminated once the convergence occurs. This can be achieved by using a stopping criterion. Many ideas have been introduced in the literature to define the conditions that should be followed to decide when convergence has occurred. Most of these techniques are introduced in Hashim and Salam (2019) and are defined as follows:

- **Iteration number:** This criterion is the regular termination of the code in many applications, but it does not guarantee complete convergence because it terminates the execution of the code once the total number of iterations is achieved.
- **Best fitness threshold:** This type of stopping criterion depends on stopping the iterations once the fitness function reaches a predefined value.
- **Fitness convergence:** This stopping criterion ensures that all the objective function values are concentrated in the final solution. This can be done by terminating the code once the difference between the highest and lowest values is lower than a predefined tolerance. This technique has been used to terminate the outer PSO loop in this study.
- **Swarm position convergence:** This condition stops the execution of the code when the difference between the maximum and minimum values of all particles' positions in the population is less than

the predefined tolerance. This criterion can be implemented also by terminating the code when the standard deviation of the particles' positions is lower than a predefined tolerance, as shown in (8). This stopping criterion has been used in the inner PSO loop of NESTPSO.

$$Std\,(d_j^{1:SS}) \leq e_1 \tag{8}$$

where Std is the standard deviation, $d_j^{1:SS}$ is the swarm positions at iteration j, and ϵ_1 is the predefined tolerance.

4.3. Determination of failure rate

Convergence failure occurs when the PSO particles are trapped in one of the LPs. It is not easy to deduce a generalized formula to be used in judging whether the global best is the right one, unless the exact GP is well known, which is the case in this application. To enable a fair evaluation between all of these strategies, the absolute difference between the GP and the global best obtained from PSO is higher than a predefined tolerance, $\epsilon_2 = 0.001$, which will be counted as a failure occurrence.

5. Simulation results

The simulation study is divided into two different studies. The first study aims to determine the optimal control parameters and swarm size of the PSO, with different numbers of peaks of the P-V characteristics of PV systems using the proposed strategy (NESTPSO). The parameters gained from NESTPSO in the first study are used in the second study to achieve the minimum convergence time and failure rate. The results obtained from NESTPSO are compared to the values obtained from 10 well-known benchmark PSO strategies. This study will demonstrate the improvement in the performance of the PSO strategy when its parameters are obtained from NESTPSO compared to the parameters obtained from the benchmark PSO strategies.

The detailed description of the PV module is shown in Table 1 (Sunperfect 2020). The PV system consists of five modules connected in series.

5.1. Design of the power modifier system

The boost converter should be designed based on the performance parameters of the other components of the circuit and the operating range of the system (Eltamaly 2015a, 2015b; Eltamaly, Al-Saud, and Abo-Khalil 2020). The design stage of the DC–DC boost converter has been described previously (Ayop and Tan 2018; Mohan, Undeland, and Robbins 2003). The detailed system parameters used in the design of the boost converter are shown in Table 1.

Table 1. Technical specifications of the photovoltaic system used in the design stage.

Parameter	Values
Insulation	$100 \leq G \leq 1000$ W/m^2
Temperature	$-25 \leq T \leq 50$°C
Open circuit voltage	$129 \leq Voc \leq 188.1$ V
Maximum short-circuit current	7.44 A
Maximum power under NOC	919 W
Voltage at maximum power, V_{mp}	125.05 V
Current at maximum power, I_{mp}	7.349 A
Switching frequency, f_s	20 kHz
Sampling time	0.05 s
DC-link voltage	180 V

Note: NOC = normal operating conditions (1000 W/m^2 and 25°C).

To determine the optimal value of the DC-link voltage, the line–line voltage is 110 V, so the DC-link voltage can be obtained from Equation (9) (Mohan, Undeland, and Robbins 2003). Based on this equation, the DC-link voltage is chosen to be 180 V to force the three-phase PWM inverter workaround $m_a = 1.0$, for better performance and linear control.

$$V_{dc} = \frac{2\sqrt{2}}{\sqrt{3}\, m_a} * V_{LL}, \quad \text{where} \quad m_a \leq 1.0 \tag{9}$$

where m_a is the modulation index of the PWM inverter and V_{LL} is the line–line voltage of the electricity utility.

The boost converter should be designed so that it works in continuous conduction mode (CCM) in most operating conditions. The minimum inductance of the boost converter inductor to make it work in CCM is shown in formula (10) (Mohan, Undeland, and Robbins 2003). As implied by (10), the maximum inductance is a function of the duty ratio, where its value is highest when the duty ratio $d = 0.5$, which will be used in this equation. If it is required to maintain the CCM in the range between 5% (0.3945 A) and 100% (7.89 A) of the rated current, $d = 0.5$, $I_{PV} = 0.3945$ A and $V_{dc} = 180$ V, then the highest inductance required should be 2.85 mH.

$$L \geq \frac{V_{dc}}{2 f_s .\, I_{PV}} d\,(1 - d) \tag{10}$$

The minimum value of the capacitor that should be inserted in the DC-link in terms of the allowable voltage ripple can be determined from formula (11) (Mohan, Undeland, and Robbins 2003). If it is required that the highest ripple in the DC-link must not exceed 1%, then the required capacitor should be greater than 54.8 μF (where $I_{PV} = 7.89$ A, $d = 0.5$, $V_{dc} = 180$ V and $\Delta V_{dc} = 0.01$). In the simulation and experimental work, a capacitance of 60 μF is used to reduce the ripple by more than 1% in the DC-link and to compensate the ripples injected from the three-phase PWM inverter.

$$C_{out} \geq \frac{I_{PV}}{f_s . V_{dc} .\, \Delta V_{dc}} d\,(1 - d) \tag{11}$$

where ΔV_{dc} is the voltage ripple factor in the DC-link.

To reduce the ripple in the output voltage of the PV array, an input capacitor should be used (Ayop and Tan 2018). The value of the input capacitor can be obtained from formula (12) (Ayop and Tan 2018). If it is required to have a ripple in the PV output voltage not exceeding 1%, the capacitance of the input capacitor should be greater than 10.75 μF; a value of 11 μF is used in the simulation and experimental work.

The values of the elements used in the boost converter are shown in Table 2.

$$C_{in} \geq \frac{d_{\max}}{8L .\, \Delta V_{mp} . f^2} \tag{12}$$

where ΔV_{mp} is the voltage ripple factor (0.01) at the maximum power point, and $d_{\max}$ is the maximum allowable value of the duty ratio (0.98).

Table 2. Values of the elements used in the boost converter.

Parameter	Value
DC-link voltage	180 V
L	2.85 mH
C_{out}	60 μF
C_{in}	11 μF

5.2. Application of NESTPSO against number of peaks

The NESTPSO strategy has been applied to 10 different shading pattern conditions, each with a different number of peaks in the P-V curves, from one to 10. To enable a fair comparison, the same stopping criteria have been used in all cases. The simulation of each case has been performed 10,000 times (N_{av} = 10,000) to avoid the dependence of the results on the random nature of the PSO. The results obtained from this simulation study are shown in Table 3. These results show that the convergence time with 0.05 s sampling intervals varies from 1.515 to 2.4015 s for cases with one to 10 peaks. These values of convergence time are substantially lower than those obtained from all benchmark PSO strategies, as shown in the next simulation study. The relationship between the optimal swarm size and the number of peaks in the P-V curve is shown in Figure 5. The relationship between the convergence time and the number of peaks in the P-V curve is shown in Figure 6.

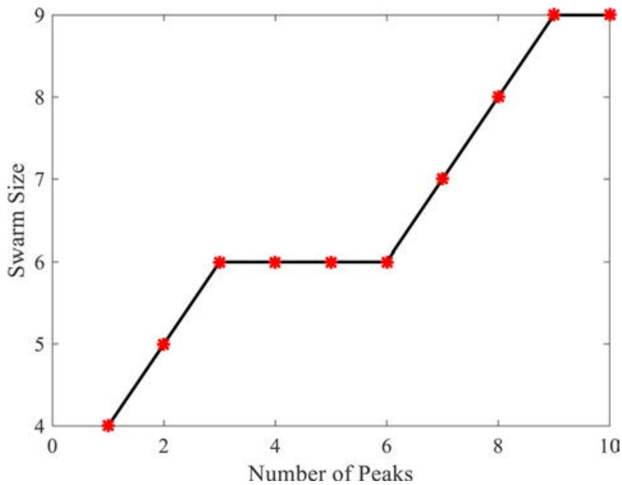

Figure 5. Relationship between the optimal swarm size and the number of peaks in the P-V curves.

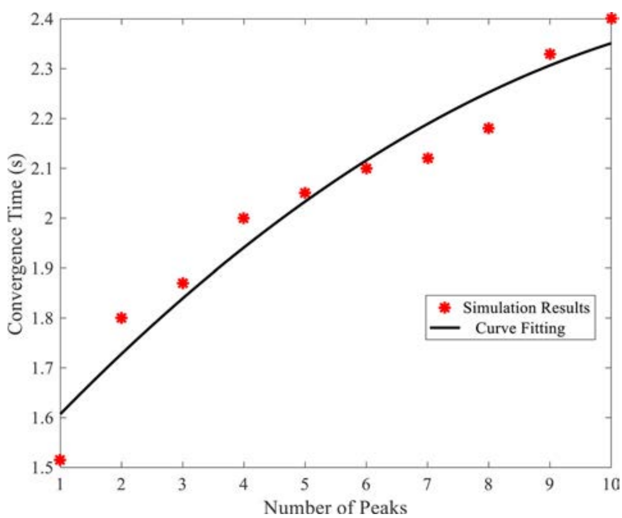

Figure 6. Relationship between the convergence time and the number of peaks.

Table 3. Simulation of the system with different numbers of peaks using the nested particle swarm optimization (NESTPSO) strategy.

No. of peaks	ω_ι	c_{li}	c_{gi}	SS_i	t_c
1	−0.0139	1.1265	0.9556	4	1.5151
2	0.2373	0.6588	1.0559	5	1.8057
3	−0.1044	−0.0794	1.4283	6	1.8706
4	0.1592	0.3463	1.1862	6	2.0347
5	0.1693	0.1177	1.2438	5	2.0502
6	0.1554	0.1555	1.2061	6	2.1008
7	0.0642	−0.0508	1.2433	7	2.1214
8	−0.0189	0.0461	1.5213	8	2.1808
9	0.0725	1.6261	1.5232	9	2.3313
10	0.0422	0.0269	1.1697	9	2.4014

Table 4. Control parameters of benchmark strategies.

Strategy	ω_ι	c_{li}	c_{gi}
S1 (Clerc and Kennedy 2002)	0.7298	1.49618	1.49618
S2 (Clerc 1999)	0.7290	1.49445	1.49445
S3 (Jiang, Luo, and Yang 2007)	0.7150	1.70000	1.70000
S4 (Mohais *et al.* 2004)	0.7290	2.05000	2.05000
S5 (Carlisle and Dozier 2001)	0.7290	2.04120	0.94770
S6 (Zhang *et al.* 2014)	0.7240	1.46800	1.46800
S7 (Clerc 2006)	0.7200	1.10800	1.10800
S8 (Liu 2015)	0.4200	1.55000	1.55000
S9 (Harrison, Engelbrecht, and Ombuki-Berman 2017)	0.5000	1.90000	1.90000
S10 (Harrison, Engelbrecht, and Ombuki-Berman 2017)	0.6000	1.80000	1.80000

5.3. Comparison of NESTPSO to the benchmark PSO strategies

The results obtained from NESTPSO are compared to 10 benchmark PSO strategies (Carlisle and Dozier 2001; Clerc 1999, 2006; Clerc and Kennedy 2002; Harrison, Engelbrecht, and Ombuki-Berman 2017; Jiang, Luo, and Yang 2007; Liu 2015; Mohais *et al.* 2004; Zhang *et al.* 2014). The control parameters of the benchmark PSO strategies are shown in Table 4. To enable a fair comparison between all benchmark PSO strategies, the swarm size is chosen to be the same ($SS_i = 6$), while the swarm size of NESTPSO is chosen as the optimal number obtained from Table 3.

Table 5 shows the results obtained using benchmark PSO strategies compared to the results obtained by NESTPSO. Some strategies show a very slow response, such as strategy S4 (Mohais *et al.* 2004), which takes a long time to converge (11.6–14.088 s). This means that this strategy is not suitable for use as an MPPT in PV systems. Some of the benchmark strategies show very short convergence times compared to the others, such as strategy S8 (Liu 2015), which captured the GP in 3.542–8.171 s. This means that this strategy is a better choice for an MPPT of PV system applications than the other benchmark PSO strategies shown in Table 5.

The results in Table 5 show that the convergence time from NESTPSO is lower than that from all other benchmark strategies. Its convergence time ranges from 1.515 to 2.0415 s, which means that it has a reduction in convergence time of 77–681% compared to the benchmark strategies shown in Table 5. It can also be seen from Table 5 that the lowest reduction in convergence time obtained using the NESTPSO strategy is 77%, when compared to strategy S8 (Liu 2015) with a six-peak shading pattern. Meanwhile, the highest reduction in convergence time using the NESTPSO strategy is 681%, when compared to strategy S4 (Mohais *et al.* 2004) with uniform distributed irradiance (one peak). These results show clearly the great reduction in convergence time when using the NESTPSO strategy for all numbers of peaks compared to the benchmark strategies. This great achievement proves the superiority of the NESTPSO strategy in determining the optimal control parameters of PSO when it is used as an MPPT in PV systems. For this reason, it is recommended that all researchers, experts and designers use these values of PSO control parameters and swarm size when PSO is used as an MPPT

Table 5. Convergence time corresponding to each benchmark strategy compared to the results from nested particle swarm optimization (NESTPSO).

	No. of peaks									
Strategy	1	2	3	4	5	6	7	8	9	10
S1	8.1225	8.2875	8.9440	8.9640	8.7170	8.0605	10.8050	9.6525	10.0310	9.5270
S2	8.2610	8.3765	8.3870	8.9090	8.9970	8.1450	11.3030	9.3130	9.6730	8.9240
S3	8.6895	9.3485	9.3770	9.7150	9.3190	8.6175	11.3480	10.3070	10.6150	9.7870
S4	11.829	12.1420	11.771	12.513	12.510	11.600	13.9540	14.0880	13.5910	13.070
S5	8.5570	9.3670	10.3220	9.1580	9.1250	8.8550	10.6970	9.8645	10.2520	9.7540
S6	7.8825	8.1020	8.1820	8.5190	7.9520	7.6190	10.2600	9.2420	9.7910	9.0070
S7	6.7545	6.8210	7.0900	7.1500	6.8430	6.4580	10.0130	7.4390	7.9860	6.8040
S8	3.5420	3.9210	4.1960	3.8620	3.9650	3.7135	8.1710	4.4965	4.9410	4.8660
S9	5.3675	5.9440	6.1700	6.2560	6.0150	5.6660	8.0680	6.6085	7.1750	6.2290
S10	6.6520	6.8130	6.7600	6.8730	7.3210	6.6185	9.8270	8.1910	8.3270	7.5240
NESTPSO	1.5150	1.8056	1.8707	2.0348	2.0501	2.1009	2.1213	2.1807	2.3312	2.4015
Max. reduction (%)	681	575	530	526	510	452	558	546	483	445
Min. reduction (%)	134	118	124	93	93	77	285	106	112	103

in PV systems. It is also clear that NESTPSO can easily determine the optimal control parameters of PSO or other soft computing optimization techniques for any application with no need for tuning, review work or expert assistance.

6. Experimental work

To validate the superior operation of NESTPSO, an experimental set-up is established. This experimental set-up has been used to measure the convergence times of different strategies. The experimental work is divided into two subsections: the hardware set-up and the experimental results.

6.1. Hardware set-up

The hardware of the PV system is set up as shown in Figure 1. A photograph the testbed system is shown in Figure 7. In Figure 7, five PV modules are connected in series and their terminals are connected to the input of the boost converter. The three-phase inverter input is connected to the DC-link of the PV system. The output of the inverter is connected to the utility grid terminals. The MPPT of the PV system is used to control the PV array terminal voltage using the duty ratio of the boost converter, which is implemented using PSO MPPT, and the second controller is used to control the three-phase PWM using the decoupling control strategy introduced by Lakshmi and Hemamalini (2018).

The control systems are implemented in MATLAB/Simulink tools and the signal values are transferred to a dSPACE (DS1104 interface card) and a real-time interface circuit. The switch used in the boost converter is a MOSFET 2SK3635 (findchips 2020), which has 200 V drain to source voltage and an 8 A drain current. A 74HC14 gate driver is used in the experimental set-up to provide an interface between the MOSFET and the control circuit. The boost converter parameters are shown in Table 2. The same five series-connected PV modules used in the simulation are used in the experimental set-up. Partial shading is achieved by covering the targeted module with semi-transparent sheets.

6.2. Experimental results

The circuit shown in Figure 1 was set up in the laboratory as shown in Figure 7, to validate the results obtained from the NESTPSO strategy compared to those obtained from one of the benchmark strategies shown in Tables 4 and 5. Four sheets with different transparencies were used to obtain five peaks in the P-V characteristics of the PV array. The experiment was conducted for two different cases:

Figure 7. Picture of the experimental set-up.

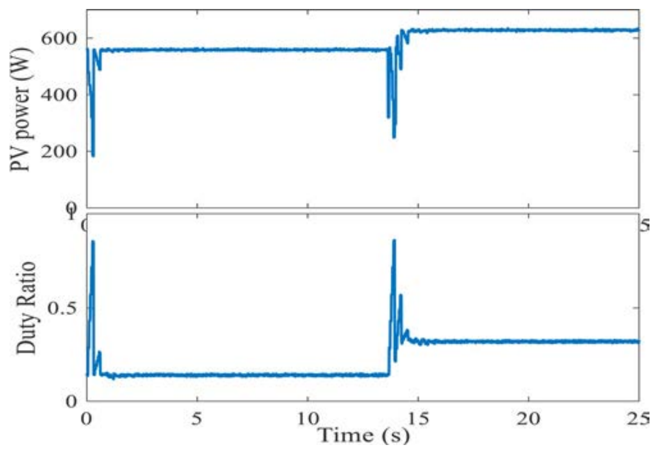

Figure 8. Experimental results obtained using the control parameters and swarm size from nested particle swarm optimization (NESTPSO). PV = photovoltaic.

Case 1. The PSO control parameters obtained from NESTPSO for five peaks are used to show the convergence time.

Case 2. The parameters used in S10 (Harrison, Engelbrecht, and Ombuki-Berman 2017) with six swarm sizes are used as an example for one of the benchmark strategies.

The results for these two cases are shown in Figures 8 and 9. The results of Case 1 are shown in Figure 8, where the optimal PSO control parameters and optimal swarm size obtained from the NESTPSO strategy are introduced to the online PSO MPPT. These values are $\omega = 0.1692$, $c_l = 0.1178$, $c_g = 1.2437$ and swarm size = 5. The experimental results for Case 1 are shown in Figure 8 for 25 s, where the control system captured the GP in about 2 s; after removal of the transparent covers the system was reinitialized and it again captured the GP after 2 s.

In Case 2, strategy S10 (Harrison, Engelbrecht, and Ombuki-Berman 2017) was used, with $\omega = 0.6$, $c_l = 1.8$, $c_g = 1.8$ and swarm size = 6. The results of Case 2 are shown in Figure 9. It can

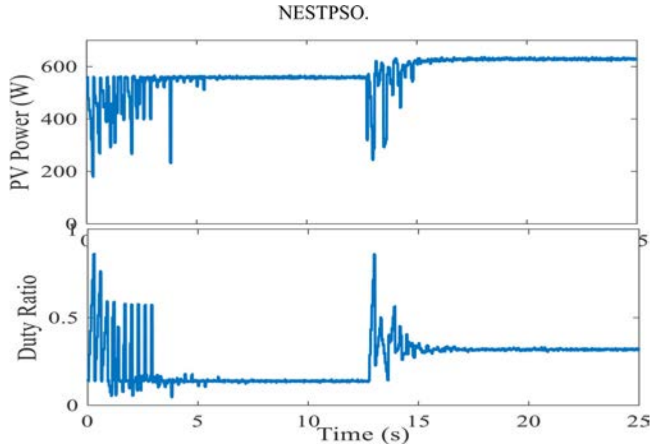

Figure 9. Experimental results obtained from the particle swarm optimization (PSO) maximum power point tracker (MPPT) of photovoltaic (PV) systems with control parameters of S10.

be seen from Figure 9 that the PSO captured the GP after 6 s; after the shading pattern changed at 13 s, the system was reinitialized and again the PSO captured the GP after 6 s.

It is clear from the experimental results that the MPPT that uses the PSO with control parameters and swarm size from the NESTPSO strategy is very fast in capturing the GP compared to the other benchmark strategies, such as S10 (Harrison, Engelbrecht, and Ombuki-Berman 2017). These results show the superiority of NESTPSO in determining the optimal PSO control parameters and swarm size when it is used as an MPPT in PV systems.

7. Conclusions and recommendations

The MPPT for PV systems under partially shaded conditions needs very fast and accurate convergence, which is not available for the conventional MPPT techniques owing to the multiple peaks generated in P-V curves. Soft computing techniques have been used to avoid this shortcoming. The PSO technique, as one of the best and most popular optimization techniques, is used for this purpose. Poor selection of PSO control parameters causes a substantial increase in failure rate and convergence time, which adversely affects the performance of the PV system, especially when used during online applications. To the author's knowledge, no previous work in the literature has determined the optimal values of control parameters and swarm size of PSO or any other soft computing technique. This article introduced a new strategy to determine these parameters and to fill this research gap. The proposed strategy, called NESTPSO, uses two nested PSO loops and places the PV MPPT as a fitness function in the inner PSO loop to optimize its PSO control parameters and swarm size. This strategy is used offline to determine these parameters, to be used later with the online application of the PSO MPPT of the PV systems. The NESTPSO strategy is performed against the number of peaks in the P-V curves to determine the optimal control parameters and swarm size for each number of peaks. The results obtained from the NESTPSO strategy were compared with 10 benchmark PSO strategies. The main finding from this comparison study is that the convergence time is reduced by between 77% and 681% compared to that associated with the benchmark PSO strategies. The results obtained from this new methodology can help researchers, designers and electricity providers in fitting PV systems on any scale. With these results, there is no need for tuning the parameters or for experts to check the performance of the PV system with different values of the PSO control parameters and swarm size. These superior results from NESTPSO open the door to further study of different online applications using PSO or any other swarm optimization technique. The same idea could be used with any soft computing technique to determine the control parameters and swarm size to optimally improve the performance of all online control applications.

Acknowledgement

The author thanks the College of Engineering Research Center and Deanship of Scientific Research at King Saud University in Riyadh, Saudi Arabia, for the financial support to carry out the research work reported in this article.

Disclosure statement

No potential conflict of interest was reported by the author.

Funding

This work was supported by College of Engineering Research Center and Deanship of Scientific Research at King Saud University in Riyadh, Saudi Arabia.

Nomenclature

d	Particle position
V_{PV}	Output voltage of the PV panels
I_{PV}	PV output current
L and C	Inductor and capacitor of boost converter
j	Iteration number of the PSO
k	Particle order within the swarm
v	Velocity of particles
P	Particle's fitness value
ω	Inertia weight
c_l, c_g	Self and social experience parameters
SS	Swarm size
it	Maximum iteration number
G_{best}	Global best position
F^k_{best}	Best fitness value of particle k
FG_{best}	Global best value of objective function
$\epsilon, \epsilon_1, \epsilon_2$	Predefined tolerances
d^k_{best}	Best position of particle k
P^k_{best}	Best value of particle k
t_s	Sampling time
N_{av}	Number of times to execute the inner loop to avoid random nature of PSO
t_c	Convergence time
FR	Failure rate
N_s	Average number of iterations consumed to achieve the peak of the inner PSO loop
N_{FR}	Number of occurrences of premature convergence
M	Weighting constant
o, i	Suffixes o and i represent the outer and inner PSO loops, respectively
PG_{best}	Global best value
r_l and r_g	Random values between [0 1]

ORCID

Ali M. Eltamaly http://orcid.org/0000-0002-9831-7182

References

Ahmed, J., and Z. Salam. 2014. "A Maximum Power Point Tracking (MPPT) for PV System Using Cuckoo Search With Partial Shading Capability." *Applied Energy* 119: 118–130.

Ayop, R., and C. W. Tan. 2018. "Design of Boost Converter Based on Maximum Power Point Resistance for Photovoltaic Applications." *Solar Energy* 160: 322–335.

Carlisle, A., and G. Dozier. 2001. "An Off-the-Shelf PSO." In *Proceedings of the Workshop on Particle Swarm Optimization*, 1–6. Indianapolis: Purdue School of Engineering and Technology.

Clerc, M. 1999. "The Swarm and the Queen: Towards a Deterministic and Adaptive Particle Swarm Optimization." *Proceedings of the 1999 Congress on Evolutionary Computation-CEC99 (Cat. No. 99TH8406), IEEE* 3: 1951–1957.

Clerc, M. 2006. Stagnation Analysis in Particle Swarm Optimisation or What Happens When Nothing Happens.

Clerc, M., and J. Kennedy. 2002. "The Particle Swarm-Explosion, Stability, and Convergence in a Multidimensional Complex Space." *IEEE Transactions on Evolutionary Computation* 6 (1): 58–73.

Eltamaly, A. M. 2015a. "Performance of Smart Maximum Power Point Tracker Under Partial Shading Conditions of Photovoltaic Systems." *Journal of Renewable and Sustainable Energy* 7 (4): 043141.

Eltamaly, A. M. 2015b. "Performance of Smart Maximum Power Point Tracker Under Partial Shading Conditions of PV Systems." *IEEE International Conference on Smart Energy Grid Engineering (SEGE)* 1: 1–8.

Eltamaly, A. M. 2018. "Performance of MPPT Techniques of Photovoltaic Systems Under Normal and Partial Shading Conditions." *Advances in Renewable Energies and Power Technologies* 1: 115–161.

Eltamaly, A. M., M. S. Al-Saud, and A. G. Abo-Khalil. 2020. "Performance Improvement of PV Systems' Maximum Power Point Tracker Based on a Scanning PSO Particle Strategy." *Sustainability* 12 (3): 1185.

Eltamaly, A. M., M. S. Al-Saud, and A. G. Abokhalil. 2020a. "A Novel Bat Algorithm Strategy for Maximum Power Point Tracker of Photovoltaic Energy Systems Under Dynamic Partial Shading." *IEEE Access* 8: 10048–10060.

Eltamaly, A. M., M. S. Al-Saud, and A. G. Abokhalil. 2020b. "A Novel Scanning Bat Algorithm Strategy for Maximum Power Point Tracker of Partially Shaded Photovoltaic Energy Systems." *Ain Shams Engineering Journal* 11 (4): 1093–1103.

Eltamaly, A M., M. S. Al-Saud, A. G. Abokhalil, and H. M. Farh. 2020. "Photovoltaic Maximum Power Point Tracking under Dynamic Partial Shading Changes by Novel Adaptive Particle Swarm Optimization Strategy." *Transactions of the Institute of Measurement and Control* 42 (1): 104–115.

Eltamaly, A. M., and H. M. H. Farh. 2019. "Dynamic Global Maximum Power Point Tracking of the PV Systems Under Variant Partial Shading Using Hybrid GWO-FLC." *Solar Energy* 177: 306–316.

Eltamaly, A. M., H. M. Farh, and A. G. Abokhalil. 2020. "A Novel PSO Strategy for Improving Dynamic Change Partial Shading Photovoltaic Maximum Power Point Tracker." *Energy Sources, Part A: Recovery, Utilization, and Environmental Effects*. doi:10.1080/15567036.2020.1769774

Eltamaly, Ali M., Hassan M. H. Farh, and Mamdooh S. Al-Saud. 2019. "Grade Point Average Assessment for Metaheuristic GMPP Techniques of Partial Shaded PV Systems." *IET Renewable Power Generation* 13 (8): 1215–1231.

Eltamaly, A. M., H. M. Farh, and M. S. A. Saud. 2019. "Impact of PSO Reinitialization on the Accuracy of Dynamic Global Maximum Power Detection of Variant Partially Shaded PV Systems." *Sustainability* 11 (7): 2091.

Farh, H. M., A. M. Eltamaly, A. B. Ibrahim, M. F. Othman, and M. S. Al-Saud. 2019. "Dynamic Global Power Extraction from Partially Shaded Photovoltaic Using Deep Recurrent Neural Network and Improved PSO Techniques." *International Transactions on Electrical Energy Systems* 29 (9): e12061.

Farh, H. M., A. M. Eltamaly, and M. F. Othman. 2018. "Hybrid PSO-FLC for Dynamic Global Peak Extraction of the Partially Shaded Photovoltaic System." *PloS One* 13 (11): e0206171.

findchips. 2020. Accessed April 13, 2020. https://www.findchips.com/detail/2SK3635/2219-NEC%20Electronics%20Group?quantity=1.

Grefenstette, J. J. 1986. "Optimization of Control Parameters for Genetic Algorithms." *IEEE Transactions on Systems, Man, and Cybernetics* 16 (1): 122–128.

Harrison, K. R., A. P. Engelbrecht, and B. M. Ombuki-Berman. 2017. "An Adaptive Particle Swarm Optimization Algorithm Based on Optimal Parameter Regions." In *Proceedings of the 2017 IEEE Symposium Series on Computational Intelligence (SSCI)*, 1–8. Piscataway, NJ: IEEE.

Hashim, N., and Z. Salam. 2019. "Critical Evaluation of Soft Computing Methods for Maximum Power Point Tracking Algorithms of Photovoltaic Systems." *International Journal of Power Electronics and Drive Systems* 10 (1): 548.

Hou, W., Y. Jin, C. Zhu, and G. Li. 2016. "A Novel Maximum Power Point Tracking Algorithm Based on Glowworm Swarm Optimization for Photovoltaic Systems." *International Journal of Photoenergy* 2016: Article ID 4910862.

Jiang, M., Y. P. Luo, and S. Y. Yang. 2007. "Particle Swarm Optimization-Stochastic Trajectory Analysis and Parameter Selection." In *Swarm Intelligence, Focus on Ant and Particle Swarm Optimization*, edited by F. T. S. Chan and M. K. Tiwari, 179–198. Vienna: Itech Education and Publishing.

Kennedy, J., and R. Eberhart. 1995. "Particle Swarm Optimization." *Proceedings of ICNN'95-International Conference on Neural Networks* 4: 1942–1948.

Lakshmi, M., and S. Hemamalini. 2018. "Decoupled Control of Grid Connected Photovoltaic System Using Fractional Order Controller." *Ain Shams Engineering Journal* 9 (4): 927–937.

Liu, Q. 2015. "Order-2 Stability Analysis of Particle Swarm Optimization." *Evolutionary Computation* 23 (2): 187–216.
Mason, K., J. Duggan, and E. Howley. 2018. "A Meta Optimisation Analysis of Particle Swarm Optimisation Velocity Update Equations for Watershed Management Learning." *Applied Soft Computing* 62: 148–161.
Mohais, A. S., A. S. Mohais, C. Ward, and C. Posthoff. 2004. "Randomized Directed Neighborhoods With Edge Migration in Particle Swarm Optimization." *Proceedings of the 2004 Congress on Evolutionary Computation (IEEE Cat. No. 04TH8753), IEEE* 1: 548–555.
Mohan, N., T. M. Undeland, and W. P. Robbins. 2003. *Power Electronics: Converters, Applications, and Design*. Hoboken, NJ: Wiley.
Premkumar, M., and R. Sowmya. 2019. "Certain Study on MPPT Algorithms to Track the Global MPP Under Partial Shading on Solar PV Module/Array." *International Journal of Computing and Digital Systems* 8 (4): 405–416.
Sangeetha, K., T. S. Babu, and N. Rajasekar. 2016. "Fireworks Algorithm-Based Maximum Power Point Tracking for Uniform Irradiation as Well as Under Partial Shading Condition." *Artificial Intelligence and Evolutionary Computations in Engineering Systems* 394: 79–88.
Sunperfect. 2020. Accessed April 13, 2020. http://www.sunperfect.com/product/polycrystalline/.
Titri, S., C. Larbes, K. Y. Toumi, and K. Benatchba. 2017. "A New MPPT Controller Based on the Ant Colony Optimization Algorithm for Photovoltaic Systems Under Partial Shading Conditions." *Applied Soft Computing* 58: 465–479.
Zhang, W., D. Ma, J.-J. Wei, and H.-F. Liang. 2014. "A Parameter Selection Strategy for Particle Swarm Optimization Based on Particle Positions." *Expert Systems with Applications* 41 (7): 3576–3584.